https://doi.org/10.5194/egusphere-2026-3184
Preprint. Discussion started: 9 July 2026


# Brief communication: Rb-Sr dating and provenance of ice-drafted dropstones from the mid-Atlantic ridge at mid-latitudes (36°12'N; 33°53'W).

Thomas Gyomlai[1], Muriel Andreani[1], Emeline Caujolle[2], Baptiste Debret[3], Valentine Puzenat-Vassor[3], Benoit Ildefonse[4] and Clémentine Fellah[1]

[1]Université Lyon 1, CNRS UMR 5276, ENS de Lyon, LGL-TPE, Villeurbanne Cedex, France
[2]Sorbonne Université, CNRS-INSU UMR 7193, Institut des Sciences de la Terre de Paris, ISTeP, Paris, France
[3]Université Paris Cité, CNRS UMR 7154, Institut de Physique du Globe de Paris, Paris, France
[4]Géosciences Montpellier, Université de Montpellier, CNRS, Montpellier, France

*Correspondence to*: Thomas Gyomlai (thomasgyomlai@aol.com)

**Abstract.** Understanding past iceberg activity during the Quaternary is key to constraining the spatial pattern and dynamics of ice sheets, as well as the amount and distribution of freshwater released during iceberg melting. These mechanisms significantly influence global climate and are primarily constrained by the records of ice-rafted deposits concentrated around ~40-50°N. The significance of iceberg transport at lower latitudes and its potential impact on the Atlantic Ocean circulation remain poorly constrained. In this study, we document three ice-rafted dropstones recovered from the Mid-Atlantic Ridge at mid-latitudes (~36°12'N), which could originate from various localities within the Laurentia or Baltica cratons. Their latitude of deposition is consistent with areas of low-iceberg concentration during Heinrich events, according to published numerical models of iceberg transport and melting. The samples form a calc-alkaline magmatic series (monzogranite, granodiorite, and tonalite) and yield in-situ Rb–Sr ages of ~1700–1630 Ma. This suggests that they derive from the Late Paleoproterozoic Labradorian arc-accretion orogeny exposed in eastern Canada. This provenance further suggests a relatively low-altitude iceberg source in the Gulf of Saint Lawrence, favoring iceberg transport to lower latitudes.

## 1 Introduction

In the North Atlantic Ocean, important volumes of ice-rafted deposits around ~40-50°N (in the subpolar gyre) have been documented, and result from the widespread discharge and melting of sediment-loaded icebergs into the ocean (e.g., Ruddiman, 1977; Heinrich, 1988; Hemming, 2004). Several periods of major iceberg discharge and large volumes of ice-rafted deposits have been identified during the Quaternary and labeled as Heinrich events (Heinrich, 1988). The locations, amounts, and provenances of these deposits have been used to study and reconstruct the spatial pattern and dynamics of ice sheets during the Quaternary (e.g., Hemming et al., 1998; Bailey et al., 2012; Thierens et al., 2012; Small et al., 2013), which are key parameters to refine climatic models (e.g., Ruddiman et al., 1989; Hemming, 2004; Raymo and Huybers, 2008; Huybers and Tziperman, 2008). In particular, the melt of numerous icebergs produces a significant input of cold freshwater to the North

https://doi.org/10.5194/egusphere-2026-3184
Preprint. Discussion started: 9 July 2026


Atlantic, which impacts the Atlantic Meridional Overturning Circulation and, in turn, induces global climate change (e.g., Broecker, 1994; Keigwin and Lehman, 1994; Oppo et al., 2015; McManus et al., 2004; Fendrock et al., 2022).

However, uncertainties remain regarding the provenance, quantity, distribution, lifespan, and impact of icebergs during Heinrich events. Past iceberg activity and associated ice-rafted deposits in the North Atlantic are primarily documented at subpolar latitudes, based on sediment core records (e.g., Hemming et al., 1998; Bailey et al., 2012; Thierens et al., 2012). Their distribution and volume are well reproduced by numerical modeling of icebergs transport and melting (e.g., Levine and Bigg, 2008; Jongma et al., 2013; Wilton et al., 2021; Fendrock et al., 2022). However, records of icebergs at latitudes below 40°N raise questions about the existence of significant short-lived ice-rafting events at lower latitudes and their potential impact on the Atlantic Ocean circulation (e.g., Condron and Hill, 2021).

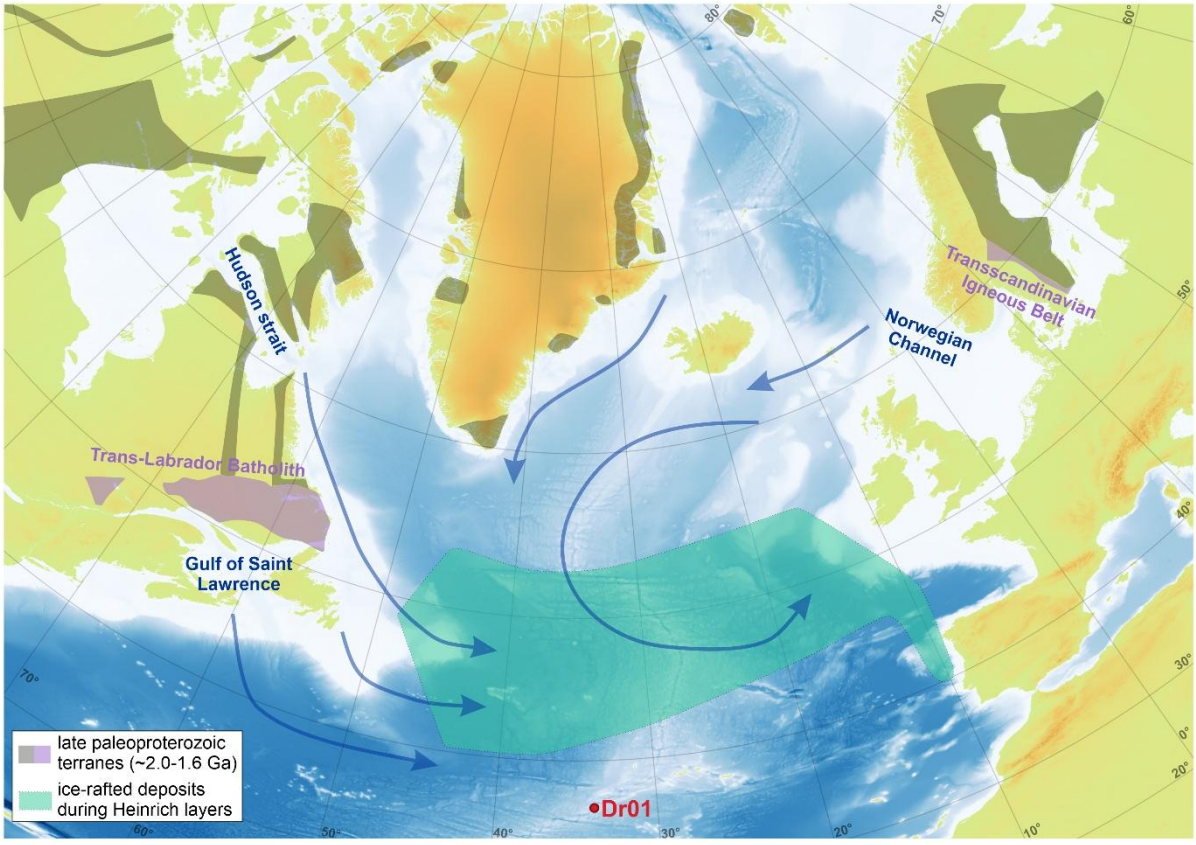


**Figure 1: Map of the North Atlantic Ocean showing the samples location (DR01) and surrounding Late Paleoproterozoic terranes (2.0-1.6 Ga) of calc-alkaline affinity shown in grey (Reed et al., 2005; Whitmeyer and Karlstrom, 2007; Lahtinen et al., 2008), and in purple when they are candidates for the source of the studied samples. The extent of documented ice-rafted deposits associated with Heinrich layers is shown in green (Ruddiman, 1977; Hemming, 2004). Arrows indicate mean iceberg pathways during the last glaciation following Bailey et al. (2012). Elevation and bathymetric data are from the GEBCO Bathymetric Compilation Group (2025).**

https://doi.org/10.5194/egusphere-2026-3184
Preprint. Discussion started: 9 July 2026


In this study, we document ice-rafted dropstones from 36°12'N on the Mid-Atlantic Ridge (MAR), which allow us to further constrain the extent of iceberg transport during the Quaternary at mid-latitudes. The three samples studied here were recovered during the 2008 MoMARDREAM cruise in dredge M8-DR01, between 36°11.70' N, 33°52.60' W and 36°11.75' N, 33°52.80' W (Fig. 1). They were first interpreted as oceanic felsic rocks and are ~10 cm subrounded to subangular pebbles associated with pelagic sediments (Andreani et al., 2014). Their relatively large size, compared to the sand-sized sediments generally found in sediment cores, allows detailed petrological and geochronological analyses, including the first application of in-situ Rb-Sr dating on dropstones, enabling provenance tracking.

## 2 Methods

The samples were analyzed using a Jeol IT800 scanning electron microscope equipped with an Oxford Instruments X-Max 50 energy-dispersive X-ray spectroscopy (EDX) detector at ENS Lyon, France, producing back-scattered-electron (BSE) images and X-ray elemental maps. Backscattered electron (BSE) imaging and X-ray elemental mapping were performed to characterize the samples. BSE images, acquired at the thin section scale, were used to estimate phase proportions and bulk-rock compositions using the volumetric masses provided by Abers and Hacker (2016). Electron microprobe (EPMA) analyses were carried out at CAMPARIS (SU-IPGP, Paris, France) using a CAMECA SX-Five instrument. Data reduction followed the method of Pouchou and Pichoir (1991). Analytical conditions for spot analyses were a 15 kV accelerating voltage, a 15 nA specimen current, and a focused beam. $Fe_2O_3$, $MnTiO_3$, garnet, $Cr_2O_3$, orthoclase, albite, apatite, fluorite, and scapolite were used as calibration standards. Representative microprobe analyses are presented in Table S1. Mineral abbreviations follow Whitney and Evans (2010). Pyroxene and amphibole structural formulas were calculated following Lindsley and Andersen (1983) and Hawthorne et al. (2012), respectively.

Rb-Sr in-situ analyses were performed at the ALIPP6 lab (ISTeP, Sorbonne University, Paris) using an imageGEO193 laser ablation system with an Agilent 8900 triple-quadrupole ICP-MS/MS coupled with a reaction cell ORS4. Analyses were performed with 50 µm spots at 8 Hz and applying a fluence of ca. 2 J/cm2 with 40 seconds of ablation. The analytical setup was optimized for maximum sensitivity in gas mode for the targeted mass isotopes in the reference material NIST610 (m/z set for the first and second quadrupoles respectively at: 85 and 85; 86 and 102 then 88 and 104). Isotopic ratios from mica were normalized to repeated analyses of the glass reference material BCR-2G with BHVO-2G and ATHO-G used as secondary reference materials to assess data quality. Both analyzed isotopic ratios of the secondary reference material are well within 5% uncertainty of the accepted value. Data reduction and instrument drift correction were performed with an in-house Matlab program (Gyomlai et al., 2022; 2023) and isochron age calculation was carried out with the IsoplotR software (Vermeesch, 2018). Results are presented in Table S2.

https://doi.org/10.5194/egusphere-2026-3184
Preprint. Discussion started: 9 July 2026


## 3 Petrography and Geochronology

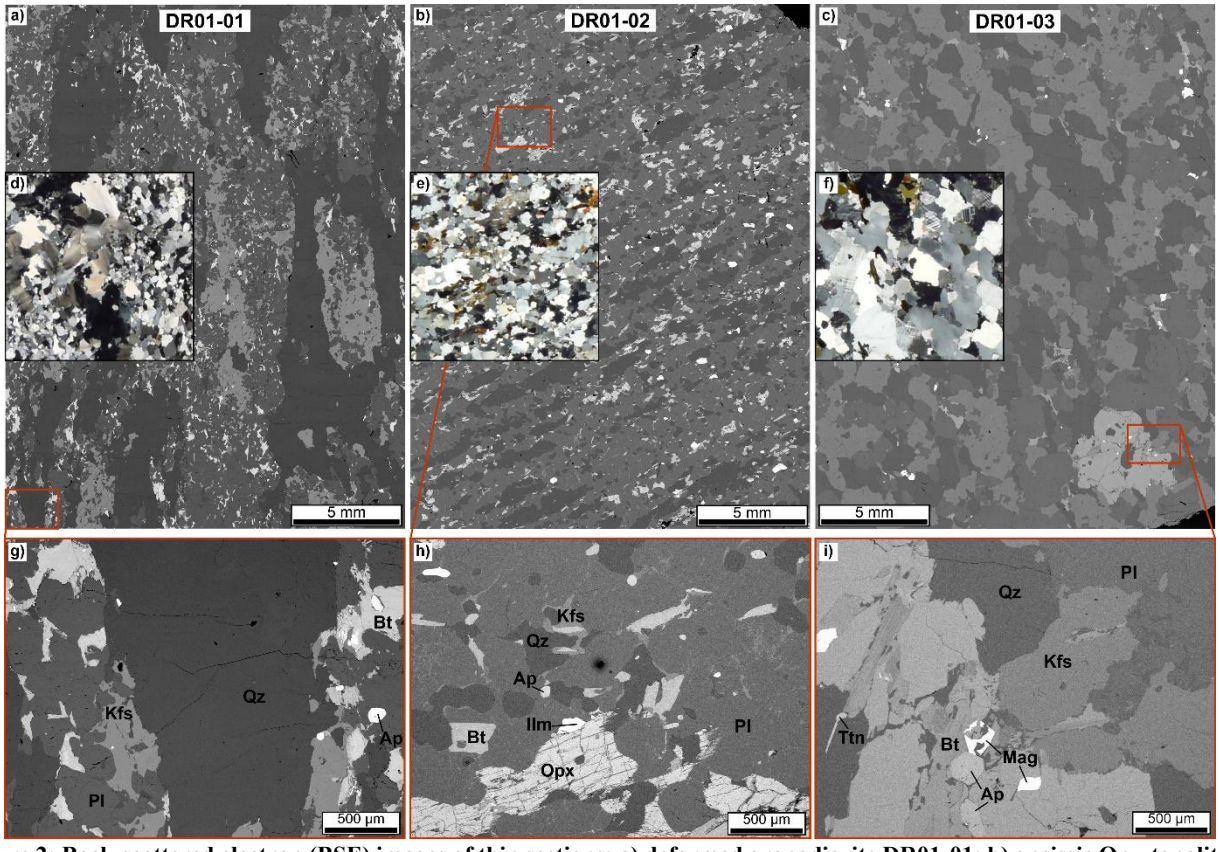


**Figure 2: Back-scattered electron (BSE) images of thin sections: a) deformed granodiorite DR01-01; b) gneissic Opx-tonalite DR01-02 and c) monzogranite DR01-03. d-f) Overlaid cross-polarized light microphotographs (same scale). g-i) Zoomed BSE images.**

M8-DR01-01 is a deformed granodiorite (following Streckeisen, 1976; Fig. 2a) composed of quartz (42.2 vol%), plagioclase (41.1 vol%; $Ab_{77-82}$ $An_{17-21}$), K-feldspar (13.0 vol%; $Ab_{04-07}$ $Kfs_{93-96}$), and biotite (3.6 vol%; XMg = 0.42-0.47; Fig. 3a), with minor (<1 vol%) zircon, muscovite (Sipfu = 3.1-3.2), epidote, fluoroapatite, and ilmenite. The calculated bulk-rock composition, expressed in oxide weight percentages (wt%), is as follows: $SiO_2$ 77.5, $TiO_2$ 0.1, $Al_2O_3$ 12.8, FeO 1.0, MgO 0.4, CaO 1.7, $Na_2O$ 4.0, $K_2O$ 2.5, corresponding to a granitic composition following Le Bas et al. (1986). The presence of plagioclase twinning, quartz undulose extinction, and quartz ribbons (Fig. 2a) suggests high-T (>350°C) solid-state ductile deformation. The overdispersion of Rb-Sr data, with a Mean Square Weighted Deviation (MSWD) of 13 for all data (Fig. 3c), indicate multiple biotite generations. A likely magmatic age is constrained at ~1700 Ma by the feldspar isochron (1697 ± 45 Ma; MSWD = 1.9; Fig. 3c) and by a large part of the analyzed biotite (orange population in Fig. 3d). A few biotite analyses may suggest an older event at ~1740 Ma (Fig. 3d), but these data are not statistically significant. A younger age population (around 1650-1630 Ma; Fig. 3d) likely represents partial resetting of biotite during high-T deformation.

https://doi.org/10.5194/egusphere-2026-3184
Preprint. Discussion started: 9 July 2026


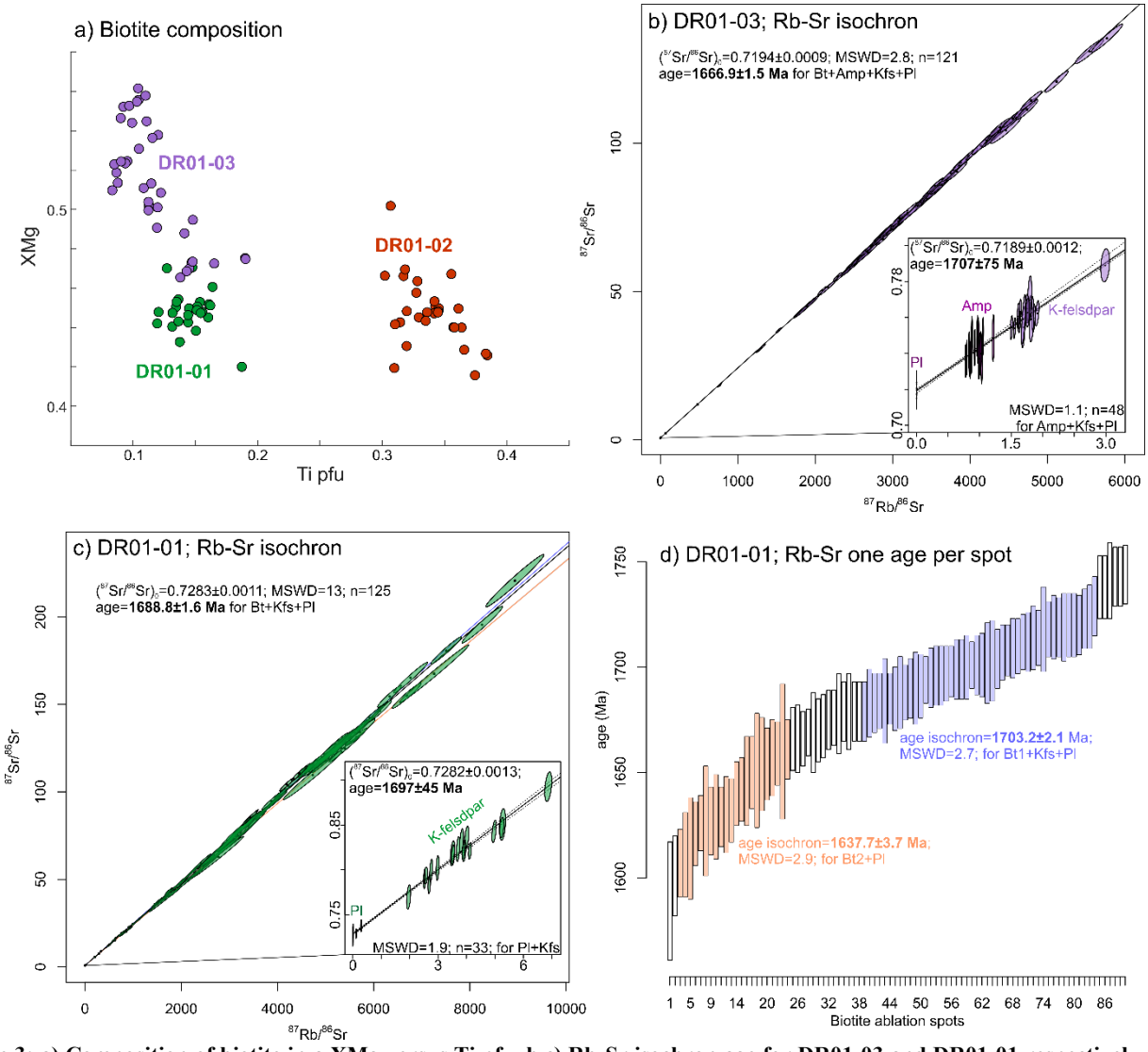


**Figure 3: a) Composition of biotite in a XMg versus Ti pfu. b,c) Rb-Sr isochron age for DR01-03 and DR01-01 respectively with a zoom on Kfs+Pl±Amp data and isochron age only from these minerals (represented by dotted lines). d) Calculated ages for DR01-01 for each ablation spot considering the initial Sr ratio given by feldspar (variability of ages depending on the chosen initial ratio on ages is <1%). Ages colored in blue and orange correspond to the two main populations of ages and isochron ages are calculated for these populations and illustrated in panel c. "n" is the number of analysed spots and all uncertainties are 2$\sigma$.**

M8-DR01-02 is a gneissic Opx-tonalite (Fig. 2b) composed of quartz (30.4 vol%), plagioclase (58.8 vol%; $Ab_{63-67}$ $An_{31-36}$ $Kfs_{01-02}$), K-feldspar (2.0 vol%; $Ab_{02-06}$ $Kfs_{94-98}$), biotite (6.0 vol%; XMg=0.42-0.50; Fig. 3a); orthopyroxene (2.0 vol%; $Wo_{01}$ $En_{39-42}$ $Fs_{57-60}$) with minor (<1 vol%) zircon, fluoroapatite, ilmenite and iron oxide. The calculated bulk rock composition (wt%) is as follows: $SiO_2$ 68.9, $TiO_2$ 0.7, $Al_2O_3$ 16.2, FeO 3.5, MgO 1.1, CaO 4.0, $Na_2O$ 4.4, $K_2O$ 1.1; corresponding to a granodioritic composition following Le Bas et al. (1986). This sample is foliated (Fig. 2b), indicating high-T deformation

https://doi.org/10.5194/egusphere-2026-3184
Preprint. Discussion started: 9 July 2026


similar to sample DR01-01. K-feldspar is sometime found at the contact between quartz and plagioclase but is mainly associated with partly rounded biotite forming coronitic textures around it, and in contact with plagioclase or quartz (Fig. 2b). This feature may suggest local partial melting potentially associated with the high-T deformation.

M8-DR01-03 is a monzogranite composed of quartz (32.1 vol%), plagioclase (29.3 vol%; $Ab_{69-73}$ $An_{22-29}$ $Kfs_{01-02}$), K-feldspar (32.7 vol%; $Ab_{05-12}$ $Kfs_{88-95}$), biotite (3.0 vol%, XMg=0.47-0.56; Fig. 3a), amphibole (2.4 vol%) and minor (<1 vol%) epidote, titanite, fluoroapatite and iron oxide. Amphibole is hastingsitic and relatively potassic ($K_{pfu}$=0.26-0.30) and magnesian ($Mg/(Mg+Fe^{2+})$=0.50-0.53), with $Ti_{pfu}$=0.14-0.16. The calculated bulk rock composition (wt%) is as follows: $SiO_2$ 72.6, $TiO_2$ 0.1, $Al_2O_3$ 14.2, FeO 2.1, MgO 0.7, CaO 2.1, $Na_2O$ 2.8, $K_2O$ 5.4; corresponding to a high-K granitic composition following Le Bas et al. (1986). This sample is coarse grained with macrocrystalline magmatic textures (Fig. 2c). Rb-Sr data obtained on biotite, K-feldspar, plagioclase and amphibole are highly consistent (Fig. 3b) with a MSWD of 2.8 and yielding a well constrained age at 1666.9±1.5 Ma.

## 4 Discussion

The three studied felsic samples were dredged at the MAR (36°12'N; Fig. 1), on the young seafloor (<0.78 Ma; Paulatto et al., 2015) of the Rainbow Massif (Andreani et al., 2014). Their two Late Paleoproterozoic ages (~1700-1630 Ma) demonstrate that they are allochthonous, and were deposited as dropstones (Bennett et al., 1994) on the active MAR during the Quaternary. This explains their exotic composition for an oceanic setting, notably their higher potassium content ($K_2O$>1wt%) compared to most oceanic felsic rocks (Koepke et al., 2007). The nature (felsic), size (~10 cm), and location (mid-Atlantic) of the three samples are indicative of transport by ice-rafting, despite not being faceted or striated (Bennett et al., 1994). Therefore, the studied samples likely originate from the Laurentia (North America and Greenland) or Baltica (Northeast Europe) cratons (Fig. 1). Considering their lithological coherence, their rarity (no previously described dropstones in the Rainbow area), and the similar ages of the two dated samples, the three studied samples are likely from the same provenance. They represent a ±K-rich calc-alkaline magma series (tonalite-granodiorite-monzogranite), typical of continental-arc batholiths in active-margin settings but also compatible with collisional orogens (Barbarin, 1999).

Figure 1 illustrates the various Late Paleoproterozoic (2.5-1.6 Ga) terranes with calc-alkaline affinity that could be the source of the studied samples (Reed et al., 2005; Whitemeyer and Karlstrom, 2007; Lahtinen et al., 2008). Most of these terranes within the Laurentia and Baltica cratons correspond to accreted calc-alkaline batholiths that contain lithologies similar to our studied samples, but only a few are younger than 1.8 Ga (Reed et al., 2005; Whitmeyer and Karlstrom, 2007; Lahtinen et al., 2008):

- In Northeast Europe, a possible candidate is from the Fennoscandian craton and corresponds to the youngest calc-alkaline magmatic rocks (1.71-1.66 Ga) of the Transscandinavian Igneous Belt (Fig. 1), associated with the Gothian orogen (Högdahl

https://doi.org/10.5194/egusphere-2026-3184
Preprint. Discussion started: 9 July 2026


et al., 2004; Lahtinen et al., 2008). However, these rocks represent a relatively small outcrop area and display more alkaline compositions than the studied samples (Högdahl et al., 2004).

- In Greenland, we identified no suitable candidate for the provenance of the studied samples. The region is divided into three roughly E-W-striking Paleoproterozoic orogenies, the youngest and southernmost of which (the Ketilidian orogen) is dated at ~1.8 Ga (Reed et al., 2005; Lahtinen et al., 2008).

- In North America, the Trans-Labrador Batholith (Canada, in the Quebec and Labrador regions; Fig. 1) experienced significant plutonism, deformation and metamorphism during the Labradorian arc-accretion orogeny (1710-1600 Ma) and matches both the lithologies (i.e., gneissic tonalites, granitoids, and monzogranites) and the obtained ages (Gower, 1996; Dickin, 2000; Whitmeyer and Karlstrom, 2007; Gower et al., 2008). We therefore consider this batholith the most plausible source for the studied dropstones.

Modelling of icebergs transport and melting in the North Atlantic mainly focuses on an iceberg source from the Laurentide Ice Sheet and the Hudson Strait ice stream (Jongma et al., 2013; Wagner et al., 2018; Condron & Hill, 2021; Fendrock et al., 2022) or from the European Fennoscandian and British-Irish Ice Sheets (Levine and Bigg, 2008; Wilton et al., 2021). In both cases, these studies suggest a very low concentration of icebergs at latitudes below 40°N, but indicate possible iceberg transport up to the Gulf Stream (~35°N). Nonetheless, southern iceberg calving from the Gulf of Saint Lawrence ice stream would favor transport and melting at lower latitudes (Levine and Bigg, 2008). Furthermore, this hypothesis is consistent with the proposed provenance of the studied dropstones from the Trans-Labrador Batholith, located just north of the Gulf of Saint Lawrence (Fig. 1). Transport of icebergs to subtropical latitudes (20–40°N) has also been documented along the American east coast (Condron and Hill, 2021) and interpreted as resulting from coastal boundary currents, which cannot account for the position of the studied dropstones in the middle of the Atlantic Ocean. Therefore, in this study we document the transport and melting of icebergs at relatively low latitude (36°N), suggesting a significant iceberg source from the Gulf of Saint Lawrence ice stream, which could represent substantial iceberg transport at latitudes lower than 40°N, with associated freshwater release and a potentially different impact on global climate.

## 5 Conclusion

In this study, we document three ice-rafted dropstones recovered at the Mid-Atlantic Ridge at mid-latitudes (36°12'N). They represent a Late Paleoproterozoic calc-alkaline magma series (monzogranite, granodiorite, and tonalite) that possibly derives from the Labradorian arc-accretion orogeny, now outcropping in eastern Canada. Their latitude of deposition is compatible with modelled low-concentration iceberg zones during Heinrich events, but is more consistent with an iceberg source from the relatively southern Gulf of Saint Lawrence ice stream. This study documents an episode of iceberg transport at relatively low latitude (36°N), suggesting transient episodes of far-reaching iceberg drift and a potentially stronger impact on ocean cooling at mid-latitudes.

https://doi.org/10.5194/egusphere-2026-3184
Preprint. Discussion started: 9 July 2026


## Data Availability Statement

The data used in this manuscript are available in appendix. Table S1 reports representative EMP mineral analyses (wt%), and Table S2 reports the Rb–Sr geochronology results.

## Author contributions

TG and MA conceptualized the study using resources provided by MA and BI. TG, EC, CF, and VP carried out the analyses. TG prepared the manuscript with contributions from all co-authors.

## Acknowledgements

This study was funded by the ANR DHYAM project (ANR-23-CE01-0011-01) obtained by M. Andreani. We thank N. Rividi, W. Bai, B. Caron and J. Noël for technical and analytical support. The authors thank J. Warren for stimulating discussions and suggestions. We thank the reviewers and editors for their comments and editorial handling.

## References

Abers, G. A. & Hacker, B. R. (2016). A MATLAB toolbox and Excel workbook for calculating the densities, seismic wave speeds, and major element composition of minerals and rocks at pressure and temperature, Geochem. Geophy. Geosy., 17, 616-624, https://doi.org/10.1002/2015GC006171

Andreani, M., Escartin, J., Delacour, A., Ildefonse, B., Godard, M., Dyment, J., Fallick, A., & Fouquet, Y. (2014). Tectonic structure, lithology, and hydrothermal signature of the Rainbow massif (Mid-Atlantic Ridge 36° 14′ N). Geochemistry, Geophysics, Geosystems, 15(9), 3543-3571. https://doi.org/10.1002/2014GC005269

Barbarin, B. (1999). A review of the relationships between granitoid types, their origins and their geodynamic environments. Lithos, 46(3), 605-626. https://doi.org/10.1016/S0024-4937(98)00085-1

Bailey, I., Foster, G. L., Wilson, P. A., Jovane, L., Storey, C. D., Trueman, C. N., & Becker, J. (2012). Flux and provenance of ice-rafted debris in the earliest Pleistocene sub-polar North Atlantic Ocean comparable to the last glacial maximum. Earth and Planetary Science Letters, 341, 222-233. https://doi.org/10.1016/j.epsl.2012.05.034

Bennett, M. R., Doyle, P., & Mather, A. E. (1996). Dropstones: their origin and significance. Palaeogeography, Palaeoclimatology, Palaeoecology, 121(3-4), 331-339. https://doi.org/10.1016/0031-0182(95)00071-2

Broecker, W. S. (1994). Massive iceberg discharges as triggers for global climate change. Nature, 372(6505), 421-424. https://doi.org/10.1038/372421a0

https://doi.org/10.5194/egusphere-2026-3184
Preprint. Discussion started: 9 July 2026


Condron, A., & Hill, J. C. (2021). Timing of iceberg scours and massive ice-rafting events in the subtropical North Atlantic. Nature Communications, 12(1), 1-14. https://doi.org/10.1038/s41467-021-23924-0

Dickin, A. P. (2000). Crustal formation in the Grenville Province: Nd-isotope evidence. Canadian Journal of Earth Sciences, 37(2-3), 165-181. https://doi.org/10.1139/e99-039

Fendrock, M., Condron, A., & McGee, D. (2022). Modeling iceberg longevity and distribution during Heinrich Events. Paleoceanography and Paleoclimatology, 37(6), e2021PA004347. https://doi.org/10.1029/2021PA004347

Gower, C. F. (1996). The evolution of the Grenville Province in eastern Labrador, Canada. Geological Society, London, Special Publications, 112(1), 197-218. https://doi.org/10.1144/GSL.SP.1996.112.01.11

Gower, C. F., Kamo, S. L., Kwok, K., & Krogh, T. E. (2008). Proterozoic southward accretion and Grenvillian orogenesis in the interior Grenville Province in eastern Labrador: Evidence from U-Pb geochronological investigations. Precambrian Research, 165(1-2), 61-95. https://doi.org/10.1016/j.precamres.2008.06.007

Gyomlai, T., Agard, P., Jolivet, L., Larvet, T., Bonnet, G., Omrani, J., Larson, K., Caron, B., Noël, J. (2022). Cimmerian metamorphism and post Mid-Cimmerian exhumation in Central Iran: Insights from in-situ Rb/Sr and U/Pb dating. Journal of Asian Earth Sciences, 233, 105242. https://doi.org/10.1016/j.jseaes.2022.105242

Gyomlai, T., Agard, P., Marschall, H. R., and Jolivet, L. (2023). Hygrochronometry of punctuated metasomatic events during exhumation of the Cycladic blueschist unit (Syros, Greece). Terra Nova, 35(2), 101-112. https://doi.org/10.1111/ter.12634

Hawthorne, F. C., Oberti, R., Harlow, G. E., Maresch, W. V., Martin, R. F., Schumacher, J. C., & Welch, M. D. (2012). Nomenclature of the amphibole supergroup. American Mineralogist, 97(11-12), 2031-2048. https://doi.org/10.2138/am.2012.4276

Heinrich, H. (1988). Origin and consequences of cyclic ice rafting in the northeast Atlantic Ocean during the past 130,000 years. Quaternary research, 29(2), 142-152. https://doi.org/10.1016/0033-5894(88)90057-9

Hemming, S. R., Broecker, W. S., Sharp, W. D., Bond, G. C., Gwiazda, R. H., McManus, J. F., ... & Hajdas, I. (1998). Provenance of Heinrich layers in core V28-82, northeastern Atlantic: 40Ar/39Ar ages of ice-rafted hornblende, Pb isotopes in feldspar grains, and Nd-Sr-Pb isotopes in the fine sediment fraction. Earth and Planetary Science Letters, 164(1-2), 317-333. https://doi.org/10.1016/S0012-821X(98)00224-6

Hemming, S. R. (2004). Heinrich events: Massive late Pleistocene detritus layers of the North Atlantic and their global climate imprint. Reviews of Geophysics, 42(1). https://doi.org/10.1029/2003RG000128

Högdahl, K., Andersson, U. B., & Eklund, O. (Eds.). (2004). The Transscandinavian Igneous Belt (TIB) in Sweden: a review of its character and evolution (Vol. 37, p. 125). Espoo: Geological Survey of Finland.

Huybers, P., & Tziperman, E. (2008). Integrated summer insolation forcing and 40,000-year glacial cycles: The perspective from an ice-sheet/energy-balance model. Paleoceanography, 23(1). https://doi.org/10.1029/2007PA001463

Jongma, J., Renssen, H., & Roche, D. M. (2013). Simulating Heinrich event 1 with interactive icebergs. Climate Dynamics, 40(5), 1373-1385. https://doi.org/10.1007/s00382-012-1421-1

https://doi.org/10.5194/egusphere-2026-3184
Preprint. Discussion started: 9 July 2026


Keigwin, L. D., & Lehman, S. J. (1994). Deep circulation change linked to Heinrich event 1 and Younger Dryas in a middepth North Atlantic core. Paleoceanography, 9(2), 185-194. https://doi.org/10.1029/94pa00032

Koepke, J., Berndt, J., Feig, S. T., & Holtz, F. (2007). The formation of SiO2-rich melts within the deep oceanic crust by hydrous partial melting of gabbros. Contributions to Mineralogy and Petrology, 153(1), 67-84. https://doi.org/10.1007/s00410-006-0135-y

Lahtinen, R., Garde, A. A., & Melezhik, V. A. (2008). Paleoproterozoic evolution of Fennoscandia and Greenland. Episodes Journal of International Geoscience, 31(1), 20-28. https://doi.org/10.18814/epiiugs/2008/v31i1/004

Le Bas, M. J., Maitre, R. L., Streckeisen, A., Zanettin, B., and IUGS (1986). Subcommission on the Systematics of Igneous Rocks: A chemical classification of volcanic rocks based on the total alkali-silica diagram, J. Petrol., 27, 745-750, https://doi.org/10.1093/petrology/27.3.745

Lindsley, D. H., & Andersen, D. J. (1983). A two-pyroxene thermometer. Journal of Geophysical Research, 88(S02), A887-A906. https://doi.org/10.1029/JB088iS02p0A887

McManus, J. F., Francois, R., Gherardi, J.-M., Keigwin, L. D., & Brown-Leger, S. (2004). Collapse and rapid resumption of Atlantic meridional circulation linked to deglacial climate changes. Nature, 428(6985), 834-837. https://doi.org/10.1038/nature02494

Oppo, D. W., Curry, W. B., & McManus, J. F. (2015). What do benthic δ13c and δ18o data tell us about Atlantic circulation during Heinrich Stadial 1? Paleoceanography, 30(4), 353-368. https://doi.org/10.1002/2014pa002667

Paulatto, M., Canales, J. P., Dunn, R. A., & Sohn, R. A. (2015). Heterogeneous and asymmetric crustal accretion: New constraints from multibeam bathymetry and potential field data from the Rainbow area of the Mid-Atlantic Ridge (36° 15'N). Geochemistry, Geophysics, Geosystems, 16(9), 2994-3014. https://doi.org/10.1002/2015GC005743

Pouchou, J.-L., & Pichoir, F. (1991). Quantitative analysis of homogeneous or stratified microvolumes applying the model "PAP". In Electron probe quantitation (pp. 31-75). Springer. https://doi.org/10.1007/978-1-4899-2617-3_4

Raymo, M. E., & Huybers, P. (2008). Unlocking the mysteries of the ice ages. Nature, 451(7176), 284-285. https://doi.org/10.1038/nature06589

Reed, J. C., Wheeler, J. O., Tucholke, B. E., Stettner, W. R., & Soller, D. R. (2005). Decade of North American geology geologic map of North America—Perspectives and explanation. https://doi.org/10.1130/DNAG-CSMS-v1.1

Roberts, W. H., Valdes, P. J., & Payne, A. J. (2014). A new constraint on the size of Heinrich Events from an iceberg/sediment model. Earth and Planetary Science Letters, 386, 1-9. https://doi.org/10.1016/j.epsl.2013.10.020

Ruddiman, W.F., 1977. Late Quaternary deposition of ice-rafted sand in the sub-polar North Atlantic (40-60 N). Geological Society of America Bulletin 88, 1813-1827. https://doi.org/10.1130/0016-7606(1977)88<1813:LQDOIS>2.0.CO;2

Ruddiman, W. F., Raymo, M., Martinson, D. G., Clement, B. M., & Backman, J. (1989). Pleistocene evolution: Northern hemisphere ice sheets and North Atlantic Ocean. Paleoceanography, 4(4), 353-412. https://doi.org/10.1029/PA004i004p00353

https://doi.org/10.5194/egusphere-2026-3184
Preprint. Discussion started: 9 July 2026


Small, D., Parrish, R. R., Austin, W. E., Cawood, P. A., & Rinterknecht, V. (2013). Provenance of North Atlantic ice-rafted debris during the last deglaciation—A new application of U-Pb rutile and zircon geochronology. Geology, 41(2), 155-158. https://doi.org/10.1130/G33594.1

Streckeisen, A. (1976). To each plutonic rock its proper name, Earth-Sci. Rev., 12, 1-33, https://doi.org/10.1016/0012-8252(76)90052-0

Thierens, M., Pirlet, H., Colin, C., Latruwe, K., Vanhaecke, F., Lee, J. R., ... & Henriet, J. P. (2012). Ice-rafting from the British-Irish ice sheet since the earliest Pleistocene (2.6 million years ago): implications for long-term mid-latitudinal ice-sheet growth in the North Atlantic region. Quaternary Science Reviews, 44, 229-240. https://doi.org/10.1016/j.quascirev.2010.12.020

Vermeesch, P. (2018). IsoplotR: A free and open toolbox for geochronology. Geoscience Frontiers, 9(5), 1479-1493. https://doi.org/10.1016/j.gsf.2018.04.001

Wagner, T. J., Dell, R. W., Eisenman, I., Keeling, R. F., Padman, L., & Severinghaus, J. P. (2018). Wave inhibition by sea ice enables trans-Atlantic ice rafting of debris during Heinrich events. Earth and Planetary Science Letters, 495, 157-163. https://doi.org/10.1016/j.epsl.2018.05.006

GEBCO Bathymetric Compilation Group 2025(2025). The GEBCO_2025 Grid - a continuous terrain model for oceans and land at 15 arc-second intervals. NERC EDS British Oceanographic Data Centre NOC. https://doi.org/10.5285/37c52e96-24ea-67ce-e063-7086abc05f29

Whitmeyer, S. J., & Karlstrom, K. E. (2007). Tectonic model for the Proterozoic growth of North America. Geosphere, 3(4), 220-259. https://doi.org/10.1130/GES00055.1

Whitney, D. L., & Evans, B. W. (2010). Abbreviations for names of rock-forming minerals. American Mineralogist, 95(1), 185-187. https://doi.org/10.2138/am.2010.3371

Wilton, D. J., Bigg, G. R., Scourse, J. D., Ely, J. C., & Clark, C. D. (2021). Exploring the extent to which fluctuations in ice-rafted debris reflect mass changes in the source ice sheet: A model-observation comparison using the last British-Irish Ice Sheet. Journal of Quaternary Science, 36(5), 934-945. https://doi.org/10.1002/jqs.3273